Biochimica et Biophysica Acta 1837 (2014) 63–72

Contents lists available at ScienceDirect

Biochimica et Biophysica Acta

journal homepage: www.elsevier.com/locate/bbabio

Light-harvesting complex II (LHCII) and its supramolecular organization in *Chlamydomonas reinhardtii*

Bartlomiej Drop [a,1], Mariam Webber-Birungi [b,1], Sathish K.N. Yadav [b], Alicja Filipowicz-Szymanska [c], Fabrizia Fusetti [c], Egbert J. Boekema [b], Roberta Croce [a,*]

[a] Department of Physics and Astronomy, Faculty of Sciences, VU University Amsterdam, De Boelelaan 1081, 1081 HV Amsterdam, The Netherlands
[b] Department of Biophysical Chemistry, Groningen Biological Sciences and Biotechnology Institute, University of Groningen, Nijenborgh 7, 9747 AG Groningen, The Netherlands
[c] Department of Biochemistry, Groningen Biomolecular Sciences and Biotechnology Institute, Netherlands Proteomics Centre & Zernike Institute for Advanced Materials, University of Groningen, Nijenborgh 4, 9747 AG Groningen, The Netherlands

ARTICLE INFO

Article history:
Received 29 May 2013
Received in revised form 23 July 2013
Accepted 30 July 2013
Available online 6 August 2013

Keywords:
Chlamydomonas reinhardtii
Photosynthesis
Photosystem II
Light harvesting complexes organization
Electron microscopy

ABSTRACT

LHCII is the most abundant membrane protein on earth. It participates in the first steps of photosynthesis by harvesting sunlight and transferring excitation energy to the core complex. Here we have analyzed the LHCII complex of the green alga *Chlamydomonas reinhardtii* and its association with the core of Photosystem II (PSII) to form multiprotein complexes. Several PSII supercomplexes with different antenna sizes have been purified, the largest of which contains three LHCII trimers (named S, M and N) per monomeric core. A projection map at a 13 Å resolution was obtained allowing the reconstruction of the 3D structure of the supercomplex. The position and orientation of the S trimer are the same as in plants; trimer M is rotated by 45° and the additional trimer (named here as LHCII-N), which is taking the position occupied in plants by CP24, is directly associated with the core. The analysis of supercomplexes with different antenna sizes suggests that *LhcbM1*, *LhcbM2/7* and *LhcbM3* are the major components of the trimers in the PSII supercomplex, while *LhcbM5* is part of the "extra" LHCII pool not directly associated with the supercomplex. It is also shown that *Chlamydomonas* LHCII has a slightly lower Chlorophyll a/b ratio than the complex from plants and a blue shifted absorption spectrum. Finally the data indicate that there are at least six LHCII trimers per dimeric core in the thylakoid membranes, meaning that the antenna size of PSII of *C. reinhardtii* is larger than that of plants.

1. Introduction

Photosystem II (PSII) is a multisubunit pigment–protein complex located in the thylakoid membrane of cyanobacteria, algae and higher plants. It captures and converts light into chemical energy, which is used to oxidize water and reduce plastoquinone in the light reactions of photosynthesis [1,2]. In *Arabidopsis thaliana* (*A.t.*) the largest isolated PSII supercomplex is dimeric and has a molecular weight of 1400 kDa [3]. The monomer may be composed of up to 40 different proteins, most of which are permanently part of the complex, while others are expressed or associated with it in stress conditions or during assembly and degradation [4]. In higher plants and algae, PSII is composed of two moieties: the core complex that contains all the cofactors of the electron transport chain, and the outer antenna, which increases the light-harvesting capacity of the core [5].

The PSII core complex is highly conserved in all organisms performing oxygenic photosynthesis [6–8]. The core contains the complex of the reaction center (RC, composed of D1 and D2 and cytochrome b559) that generates the redox potential required to drive water splitting [9] and the Chlorophyll (Chl) a-binding antenna complexes CP43 and CP47 [5,10]. On the luminal side of the core, several extrinsic proteins (PsbO, PsbQ, PsbP, PsbR in plants and green algae) form the oxygen-evolving complex (OEC), which supports water oxidation [9,11].

The genes encoding for the antennas of PSII of plants and green algae are members of the light-harvesting complex (Lhc) multigenic family, which also includes the antenna complexes of PSI [12]. These proteins show structural homology [13,14]: each Lhc polypeptide has three transmembrane α-helices and coordinates Chls a, Chls b, and different carotenoid molecules. In higher plant LHCII, the most abundant light-harvesting complex is composed of 3 gene products (*Lhcb1–3*) organized as heterotrimers. Each LHCII apoprotein binds eight Chls a, six Chls b and four carotenoids [13,15]. The other Chlorophyll a/b-binding proteins, *Lhcb4*, *Lhcb5*, and *Lhcb6*, also known as CP29, CP26, and CP24, exist as monomers and

* Corresponding author. Tel.: +31 20 59 86310; fax: +31 20 5987999.
E-mail address: r.croce@vu.nl (R. Croce).
[1] These authors contributed equally to this work.

0005-2728
http://dx.doi.org/10.1016/j.bbabio.2013.07.012

have different pigment compositions [16–18]. The major function of the outer antenna system is to capture light energy and transfer excitation energy to the RC [2]. However, in high light, when the absorbed energy exceeds the photosynthetic capacity and can be damaging for the system, it ensures photoprotection by the dissipation of excess energy as heat (via the process called non-photochemical quenching) to avoid formation of harmful radicals, e.g. [19,20].

In *Chlamydomonas reinhardtii* (*C.r.*) nine genes (*LhcbM1–M9*) encode LHCII proteins. Two minor antennas, CP26 and CP29, are present while CP24 is not found in the genome of this alga [21–23]. The *LhcbM* gene products have been divided into four groups based on their sequence similarity: Type I (*LhcbM3*, *LhcbM4*, *LhcbM6*, *LhcbM8*, and *LhcbM9*), Type II (*LhcbM5*), Type III (*LhcbM2* and *LhcbM7*), and Type IV (*LhcbM1*) [22,24]. Within their types, these proteins share a very high homology, i.e. sequence analysis of the Type I or Type III proteins shows up to 99% identity. Instead, the average homology between the types is lower: sequence identity between *LhcbM6* (Type I) and *LhcbM5* (Type II), *LhcbM2* (Type III), *LhcbM1* (Type IV) is 80%, 77%, and 74%, respectively [22]. Functional studies of these complexes are available only for *LhcbM2*/*7*, *LhcbM5* and *LhcbM1* [25–27] and suggest that the first two are involved in state transitions, while *LhcbM1* is important for NPQ.

The structures of several PSII components, including the cyanobacteria core [6,28], the plant LHCII trimer [13,15] and CP29 from plants [16] have been resolved at intermediate/high resolution. Information about the organization of the PSII–LHCII supercomplexes has been obtained by electron microscopy and single particle analysis [3,7,29–33] and at present the best map has a maximal resolution of 12 Å [3]. The LHCII trimers associated with the core can be distinguished in three types, based on their position in the PSII supercomplex and their strong (S), moderate (M) or loose (L) association with the core (C) [29]. The $C_2S_2M_2$ supercomplex is the largest PSII–LHCII observed in *A. thaliana* and it is composed of a dimeric core (C2), two LHCII-S trimers, interacting directly with the core and with CP29, CP26, and two M-trimers, which are associated with the core via CP29 and CP24 [3,5,29,30,32]. The position of the loosely bound trimer LHCII-L is still unclear and complexes containing one L trimer have been observed only in spinach [29].

In *C. reinhardtii* a complex with C_2S_2 organization was reported [7,34], as expected due to the absence of CP24, which in higher plants is essential for connecting trimer M to the core [35,36]. However, recently, larger PSII supercomplexes with up to 6 trimers per dimeric core were observed [33], showing that the absence of CP24 does not influence the association of trimer M with the supercomplex, and that an additional trimer is associated with the supercomplex on the side that in plants is occupied by CP24.

In order to obtain further information about the antenna complexes of PSII and their supramolecular organization in *C. reinhardtii* we have isolated different PSII sub- and supercomplexes. These complexes were characterized by combining biochemistry, spectroscopy and single particle electron microscopy. The analysis reveals the structural organization of PSII–LHCII and addresses the position and the composition of individual LHCII trimers and their role in the assembly and functioning of the supercomplex.

2. Material and methods

2.1. Strain and growth conditions

Cells of *C. reinhardtii* strain (JVD-1B[pGG1]) in which a hexahistidine tag has been added at the N-terminus of PsaA core subunit of PSI [37] were grown in liquid Tris–acetate–phosphate (TAP) medium [38] at room temperature (25 °C) on an incubator shaker (Minitron, INFORS HT) at 170 rpm under a continuous illumination flux of 20 μmol photons PAR m^{-2} s^{-1}. In those conditions the cells were in state 1.

2.2. Thylakoid preparations

Cells were harvested by centrifugation (3500 rpm, 5 min, 4 °C) at mid-logarithmic phase ($OD_{750\ nm} \approx 0.7$). *C.r.* thylakoid membranes were prepared under dim light in a cold room as described by Fischer et al. [39] with modification from Drop et al. [40]. PSII enriched membranes (BBY) from *A. thaliana* were prepared according to Berthold et al. [41] with the modifications reported by Caffarri et al. [3].

2.3. Isolation of PSII light-harvesting antenna complexes

PSII supercomplexes isolation was modified from Drop et al. [40]. Thylakoids were pelleted, unstacked with 5 mM EDTA and washed with 10 mM Hepes (pH 7.5). Membranes were then resuspended in 20 mM Hepes (pH 7.5), 0.15 M NaCl and solubilized at a final chlorophyll concentration of 0.5 mg/ml by adding an equal volume of 0.6% α-dodecyl maltoside (α-DM). Unsolubilized material was eliminated by centrifugation (12,000 rpm for 10 min at 4 °C).

To remove His-tagged PSI complexes from the preparation, the supernatant was loaded onto a HisTrap HP Column (GE Healthcare) equilibrated with 20 mM Hepes (pH 7.5), 0.15 M NaCl, and 0.03% α-DM. PSI-depleted, fraction (flow through) was loaded on a sucrose density gradient (prepared by freezing and thawing 0.5 M sucrose, 20 mM Hepes (pH 7.5), and 0.03% α-DM buffer layered over 1 ml of 2 M sucrose). PSII complexes were separated by ultracentrifugation (41,000 rpm, 14 h, 4 °C). The green bands visible on the sucrose gradient were harvested with a syringe.

The purification of PSII supercomplexes from *A.t.* was performed in the same conditions used for the purification of the *C.r.* PSII supercomplexes, with the difference that upon solubilization the membranes (BBY) were directly loaded on the sucrose gradient.

2.4. Gel electrophoresis

Proteins were analyzed by a SDS-6 M urea PAGE with Tris–sulphate buffer system prepared as discussed in Bassi [42] at a 14% acrylamide concentration. The amounts of sample loaded into each well were: 3 μg (in Chls) for thylakoids; 2.5 μg for PSII supercomplexes; and 1.5 μg for *Lhcb* fractions. The Coomassie stained gel was imaged with ImageQuant LAS-4000 (GE Healthcare).

2.5. Mass spectrometry analysis

2.5.1. In-gel tryptic digestion

For mass spectrometry-based protein identification, the SDS-PAGE bands were excised from the gel and treated with 10 mM DTT followed by 55 mM iodoacetamide in 50 mM NH_4HCO_3, to reduce and alkylate cysteine residues, and subsequently dehydrated by incubation for 5 min in 100% acetonitrile. The gel slices were rehydrated in 10 μl trypsin solution (Trypsin Gold, mass spectrometry grade, Promega10 ng/μl in 25 mM NH_4HCO_3), and incubated for 2 h at 37 °C. Subsequently 10 μl of 25 mM NH_4HCO_3 was added to prevent drying and the incubation was prolonged overnight at 37 °C. The tryptic peptides were recovered by three subsequent extractions with 50 μl of 35%, 50% and 70% acetonitrile in 0.1% TFA. The extracted peptides were pooled and concentrated under vacuum.

To determine protein composition of PSII supercomplexes, sucrose gradient fractions were first loaded on 10% SDS-PAGE and run about 1 cm through the resolving gel. This procedure was applied to clean up samples from detergent. The whole gel bands were then cut in three slices and tryptic digestion was performed as described above.

2.5.2. Liquid chromatography–mass spectrometry (LC–MS)

Fractions of the peptide mixtures from in-gel trypsin digestions were diluted in 5% formic acid, passed through a pre-column (EASY-Column C18, 100 μm × 20 mm, 5 μm particle size, Thermo Scientific, Bremen,

Germany) and separated on a capillary column (C18 PepMap 300, 75 μm × 100 mm, 3-μm particle size, Thermo, Thermo Scientific, Bremen, Germany) mounted on a Proxeon Easy-nLCII system (Thermo Scientific, Bremen, Germany). Solutions of 0.1% formic acid in water and a 0.1% formic acid in 100% acetonitrile were used as the mobile phases. A gradient from 4 to 35% acetonitrile was performed for 120 min at a flow rate of 300 nl/min. Eluted peptides were analyzed using a Linear ion Trap–Orbitrap hybrid mass spectrometer (LTQ–Orbitrap XL, Thermo Scientific). MS scans were acquired in the Orbitrap, in the range from 350 to 1800 m/z, with a resolution of 60,000 (FWHM). The 7 most intense ions per scan were submitted to MS/MS fragmentation (35% Normalized Collision Energy™) and detected in the linear ion trap.

2.5.3. Protein identification

The MS raw data were analyzed with Mascot (version 2.1, Matrix Science, London, UK) using the Proteome Discoverer 1.3 analysis platform (Thermo Scientific) and searched against the *C.r.* proteome. Peptide tolerance was set to 10 ppm and 2.0 Da for intact peptides and fragment ions respectively, using semi-trypsin as protease specificity and allowing for up to 2 missed cleavages. Oxidation of methionine residues, deamidation of asparagine and glutamine, and carbamidomethylation of cysteines were specified as variable modifications. The MS/MS based peptide and protein identifications were further validated with the program Scaffold (version Scaffold 4.0, Proteome Software Inc., Portland, OR). Protein identifications based on at least 2 unique peptides identified by MS/MS, each with a confidence of identification probability higher than 95%, were accepted.

2.6. Pigment composition

The chlorophyll concentrations of thylakoid preparations were calculated in 80% (v/v) acetone, according to Porra et al. [43].

The pigment composition of the complexes was analyzed by fitting the spectrum of the 80% acetone extracted pigments with the spectra of the individual pigments in acetone and by HPLC, as described previously [17]. As shown by Angeler and Schagerl [44], loroxanthin was eluted just after neoxanthin, but in our experimental setups the separation of these two was not possible: both carotenoids resulted in single peak. The data are the results of at least four different preparations in two replicas.

2.7. Spectroscopic analysis

Room temperature absorption spectra were recorded with a Cary 4000 spectrophotometer (Varian).

The fluorescence emission spectra were recorded at 5 °C at low temperature (77 K) using a Fluorolog 3.22 spectrofluorometer (Jobin Yvon-Spex). For 77 K measurements a home built liquid nitrogen cooled device was used. The excitation wavelengths were 440 nm, 475 nm and 500 nm and emission was detected in the 600–800 nm range. Excitation and emission slits bandwidth were set to 3 nm. All fluorescence spectra were measured at OD 0.05 at the maximum of the Qy absorption. Room temperature measurements were performed in 0.5 M sucrose, 20 mM Hepes (pH 7.5), and 0.03% α-DM buffer. For low-temperature measurements, samples were in 66.7% glycerol (w/v), 20 mM Hepes (pH 7.5), and 0.03% α-DM buffer.

2.8. Electrochromic shift (ECS)

PSI/PSII ratio of *Chlamydomonas* cells was measured with a Joliot-type spectrophotometer [45] (Bio-Logic SAS JTS-10) as described previously [46,47]. A PSI/PSII ratio of 0.97 ± 0.2 was obtained.

2.9. Electron microscopy and single particle analysis

Samples were negatively stained using the droplet method with 2% uranyl acetate on glow discharged carbon-coated copper grids. Electron microscopy was performed on a Philips CM120 electron microscope equipped with a LaB6 filament operating at 120 kV. Images were recorded with a Gatan 4000 SP 4K slow-scan CCD camera at 130,000× magnification at a pixel size (after binning the images) of 2.25 Å at the specimen level with GRACE software for semi-automated specimen selection and data acquisition [48]. Single particle analysis was performed using GRIP software including multi-reference and non-reference alignments, multivariate statistical analysis, and classification, as in Boekema et al. [29].

To determine the angle of rotation of the trimers: 1) in GRIP, all three trimers were selected at their midpoints, boxed out of the complex projections and aligned to their 3-fold rotationally averaged projections before aligning with S-trimer as reference, and 2), in comparison, PowerPoint (Microsoft) was used to draw a triangle as a reference around the reference trimer. Copies of this triangle were then rotated to align with the other trimers and the angle by which the triangle was rotated was determined in the program.

To model the supramolecular organization of the supercomplex, the available crystal structures of the cyanobacterial PSII core [6] (3ARC), LHCII trimer [13] (1RWT) and CP29 [16] (3PL9) were used. PyMOL was used to construct an aligned complex model.

3. Results

3.1. Isolation of PSII supercomplexes

To purify the PSII–LHCII complexes of *C. reinhardtii* the procedure described before for higher plants [3] was modified. Since it is not possible to prepare grana membranes from *C. reinhardtii*, as the presence of PSI interferes with the purification of PSII supercomplexes, we have used a strain carrying a hexa-histidine tag at the N-terminus of the core subunit PsaA [37,40]. The thylakoid membranes purified from this strain were mildly solubilized, to keep the large PSII supercomplexes intact, and loaded on a Ni-Sepharose column to eliminate PSI. To obtain homogeneous preparations of PSII sub- and super-complexes with different antenna sizes, the flowthrough fraction was subjected to sucrose density gradient ultracentrifugation. The gradient separation resulted in one yellow band (B1, containing free pigments), eight green bands (B2–B9), containing protein–chlorophyll complexes, and a fraction of partially unsolubilized material laying on top of the 2 M sucrose solution (B10) (Fig. 1A). The band pattern was very similar to that obtained from the solubilization of the grana membrane of *A. thaliana*, characterized before [3], suggesting the presence of PSII sub- and supercomplexes. As expected, the band corresponding to the *A.t.* CP24/CP29/LHCII-M complex ("band 4") was absent in *C. reinhardtii*, due to the lack of CP24.

The polypeptide composition of fractions B2–B9 was analyzed by SDS-PAGE (Fig. 1B), showing the presence of PSII components in all fractions. The exact protein composition of the most prominent gel bands was confirmed by mass spectrometry. The results of the analysis are summarized in Fig. 1.

Fraction B2, which mobility in the gradient corresponds to monomeric *Lhcb*, contains CP26 and CP29, and LHCII (mainly *LhcbM1*, *LhcbM2/M7* and *LhcbM3*), while fraction B3 contains the trimeric complexes. It was suggested that the trimeric form of *C.r.* LHCII is less stable than that of plants and may partly dissociate into monomers upon treatment with detergents [49]. This can explain the high content of LHCII in fraction B2 and the higher abundance of monomeric complexes (B2) compared to trimeric (B3) (Fig. 1A, B). However, it should be mentioned that when solubilized thylakoids were directly loaded on the sucrose gradient, the trimeric fraction was far more abundant than that of monomers (data not shown) indicating that, although less stable than in plants,

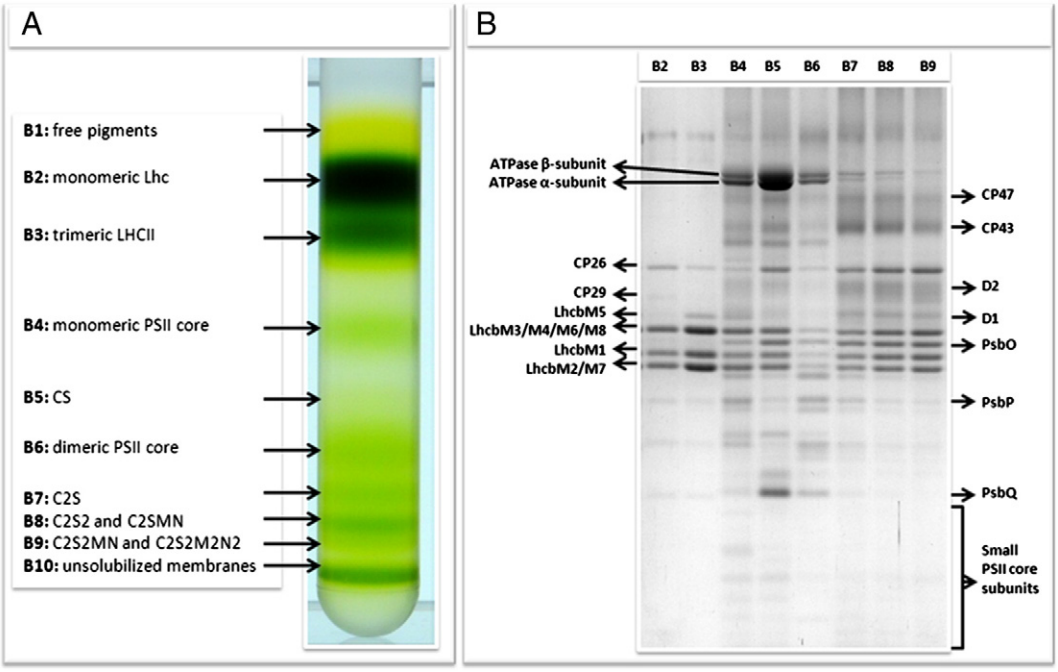

Fig. 1. Purification of PSII sub- and supercomplexes. Panel A: fractionation of PSII sub/super-complexes by sucrose density gradient. Panel B: SDS-PAGE analysis of fractions B2–B9 from sucrose gradient. Proteins identified by mass spectrometry are indicated.

almost all of the *LhcbMs* are present as trimers in the membrane. The *LhcbM* protein composition of B2 and B3 was very similar with the exception of *LhcbM5*, which was only present in B3, suggesting that trimers containing *LhcbM5* are relatively stable. Interestingly, CP26, which in plants exists as a monomer, could be observed mainly in fraction B3. There are two possible explanations: CP26 forms homo or hetero-trimers in *C. reinhardtii*, or it is strongly associated with a LHCII trimer.

The polypeptide composition of fraction B4 revealed the presence of PSII core subunits but also of LHCII and CP29. It is clear that the antenna present in this band cannot be associated with the core because the molecular weight of this band corresponds to that of PSII core monomer. This suggests that the monomeric core co-migrates with an oligomer of antenna complexes. In *A. thaliana* a complex composed of CP24/CP29/LHCII-M could be purified. In *C. reinhardtii* CP24 is absent but its position in the supercomplex is occupied by a LHCII trimer [33] (see below). It might thus be possible that a complex composed of CP29 and 2 LHCII trimers is stable enough to survive solubilization. The molecular weight of this complex would indeed be comparable to that of the monomeric core. In contrast to B4, in fraction B5 the amount of CP26 increased significantly. PSII subcomplex in B5 might consist of PSII monomeric core/LHCII-S/CP26 (CS/CP26), as was reported before for higher plants [3]. The SDS-PAGE of fractions B4 and B6 showed the presence of LHCI antenna indicating that these fractions are contaminated with PSI sub- and super-complexes, which are indeed expected to migrate at these positions [40]. The presence of PSI contamination is confirmed by the spectra which are red-shifted compared to the spectra of the other fractions (data not shown). In the upper part of the gel the bands of the α and β subunits of the ATPase are also visible. Due to their heterogeneous content bands B4–B6 were thus not analyzed further.

The protein compositions of B7, B8 and B9, which correspond to PSII supercomplexes, were very similar, while the ratio between PSII core subunits (CP47 and/or CP43) and *Lhcb* subunits decreased when going from B7 to B9, in agreement with an increased antenna size.

3.2. Electron microscopy and single-particle analysis

To determine the structural organization of PSII–LHCII, electron microscopy and single particle analysis were performed. The analysis of about 50,000 projections from fractions B7, B8 and B9 yielded six types of supercomplexes (Fig. 2A, B), in which the dimeric PSII core complex (C2) was associated with a variable number of LHCII trimers. Two LHCII trimers occupied positions equivalent to those of the S- and M-trimers in the $C_2S_2M_2$ supercomplex of *A. thaliana* [3], while the third trimer was located in the position that in *A. thaliana* is occupied by CP24, as observed before [33]. Because this trimer was directly associated with the PSII core, without involvement of any monomeric antenna, it is named trimer-N (naked). We prefer this notation to "trimer L" for two reasons: (i) trimer L has been observed only in spinach where it occupies a different position; and (ii) "L" is short for "loosely bound" [29], which is not completely appropriate for this trimer because its association to the supercomplex survives purification.

Fractions B7 and B8 contain mainly PSII dimeric core complexes with one S trimer (C_2S) and two S trimers (C_2S_2) respectively. Fraction B9 contains three types of PSII–LHCII particles, which beside LHCII-S and LHCII-M also include LHCII-N trimers: C_2SMN, C_2S_2MN and the largest complex composed of 6 LHCII trimers surrounding the dimeric core, $C_2S_2M_2N_2$. If we consider all the particles from the data set, and not only those added in the final figures because of their good image quality, the ratio of the three largest particles in B9 was about 4.5 (C_2SMN):4 (C_2S_2MN):1 ($C_2S_2M_2N_2$). This means that in the lower band the average number of trimers per dimeric core complex is about 3.7.

The projection of the C_2S_2MN supercomplex was obtained at a 13 Å resolution. This resolution allows to identify the major structural features of the individual complexes and to use them to fit the X-ray high-resolution structures of LHCII [13], CP29 [16] and PSII core [6] into the projection map of the particle. The obtained model of the supramolecular organization of the PSII supercomplex is shown in Figs. 3 and 4.

The projection maps of the C_2S_2 supercomplexes of *C. reinhardtii* and *A. thaliana* are very similar, suggesting that CP26 and CP29 occupy the same positions, with CP26 located close to CP43 and CP29 next to CP47 [3,29,32]. Trimer S is also located in the same position and it

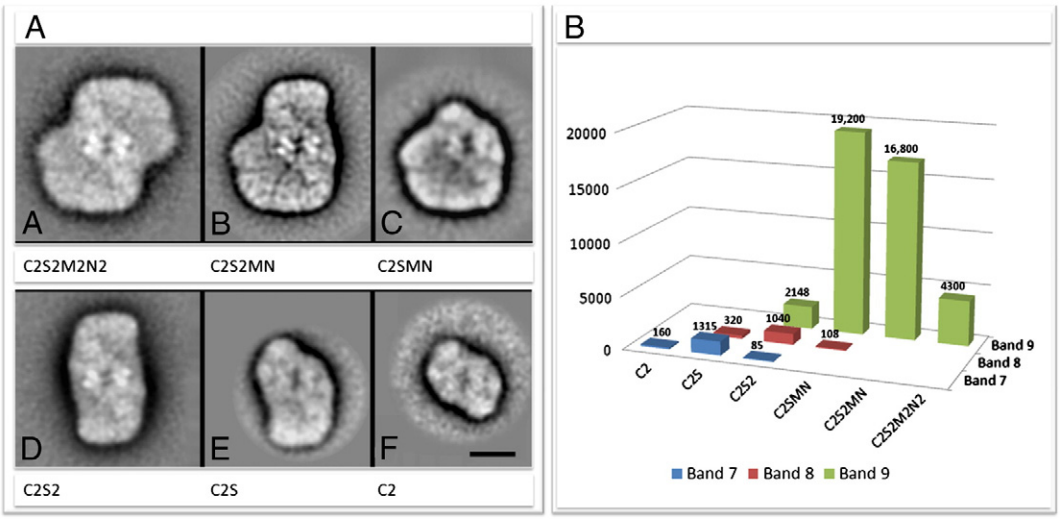

Fig. 2. Panel A: EM analysis of the *C.r.* PSII supercomplexes obtained from fractions B7–9. Averaged projection maps of PSII particles obtained by single particle averaging of about 50,000 projections. (A) $C_2S_2M_2N_2$ particle, sum of 128 projections. (B) C_2S_2MN particle, sum of 5000 projections. (C) C_2SMN particle, sum of 2000 projections. (D) C_2S_2 particle, sum of 1024 particles. (E) C_2S, sum of 512. (F) C2 core sum of 128. Notes: the map of frame B has been high-pass filtered to enhance the fine features of image processing. A two-fold rotational symmetry was imposed after processing on the map of frame A. Spacebar for all frames equals 10 nm. Panel B: numbers of projections analyzed from fractions B7, B8 and B9.

has the same orientation with respect to the core in the two supercomplexes. This is not the case for trimer M, which in *C. reinhardtii* is rotated to 45° compared to its orientation in *A. thaliana*. N-trimer is associated with the core, CP29 and trimer M and it is rotated to 25° with reference to trimer S (Fig. 4B). These values are within an accuracy of 5–10° because the trimer features are not precisely outlined by the uranyl acetate negative stain. This contrasting agent does not penetrate much inside the membrane, where the bulk of the protein is located.

3.3. Protein composition of the supercomplexes

To get information about the protein composition of the PSII supercomplexes, fractions B7–B9 were analyzed by mass spectrometry. A shotgun proteomic approach revealed the presence of all major core subunits (D1, D2, CP43, CP47) as well as of the oxygen evolving complex subunits (PsbP, PsbO, PsbR) and of some of the small core subunits (PsbE, PsbF, PsbH, PsbW) (Table S1). The other core subunits are likely to be present in PSII supercomplexes, but unidentifiable by tryptic digestion, because the resulting peptides would be too short and would not be detectable in our experimental setup. The analysis also showed the presence of CP26 (*Lhcb5*), CP29 (*Lhcb4*) and of several *LhcbM* gene products. The sequences of *LhcbM* proteins are highly homologous, and the analysis allows to identify with 100% probability (at least 2 exclusive peptides with >95% probability) *LhcbM1*, *LhcbM2*/*7* (*LhcbM2* and *M7* are practically identical and it is not possible to discriminate between the two), *LhcbM3* and *LhcbM5*, while only one peptide was identified for *LhcbM8* and *LhcbM9*. However, several peptides that are common to *LhcbM4* and *M6* were also detected, indicating that at least one of these two proteins is present in the preparation.

To determine the relative abundance of each subunit in the different fractions, spectral count normalization was applied, meaning that the spectra of each subunit (Table S1) were counted and were normalized to the spectra of D1 and D2 in the same fraction to compensate for differences in sample loading [50]. The PSII core subunit content of B7–B9 is presented in Fig. 5 normalized to the abundance of the same subunit in B9 (Table S1). The data indicate that the amount of the major core subunits – D1, D2, CP43 and CP47 – remained almost unchanged, supporting the reliability of the method.

Lhcb4 and *Lhcb5* were present in the same amount in B8 and B9 while their content was reduced in B7, in agreement with the presence

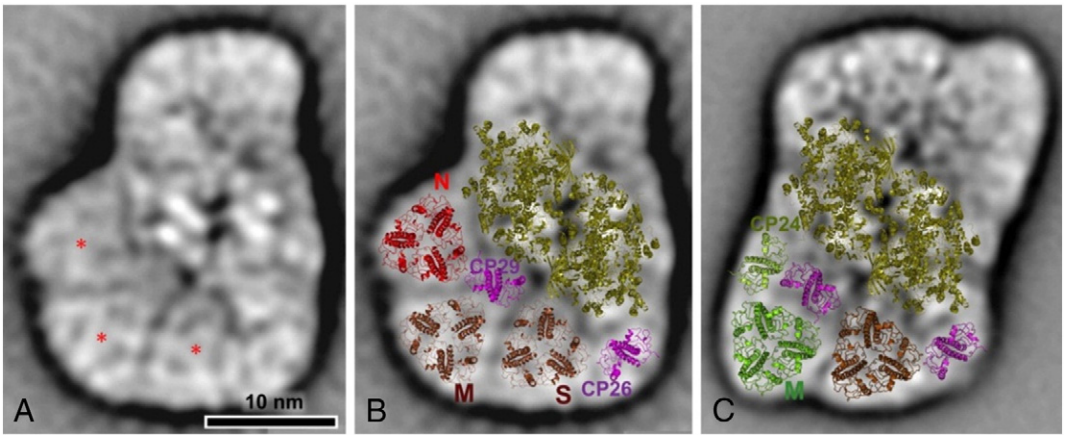

Fig. 3. Map of the *C.r.* PSII–LHCII supercomplex at a 13 Å resolution. Panel A: top view projection map of the C2S2MN supercomplex obtained from single particle electron microscopy. Panel B: assignment of the subunits in the supercomplex by fitting the high-resolution structures of PSII core [6] (in lime green), trimeric LHCII-S and LHCII-M (in brown), novel LHCII-N (in red) and monomeric *Lhcb* (in magenta) [13], and CP29 [16]. Panel C: the largest PSII–LHCII supercomplex ($C_2S_2M_2$) isolated from *A.t.* (adapted from [3]) is shown at the same scale for a direct comparison of the PSII antenna size between green algae and higher plants. Spacebar equals 10 nm.

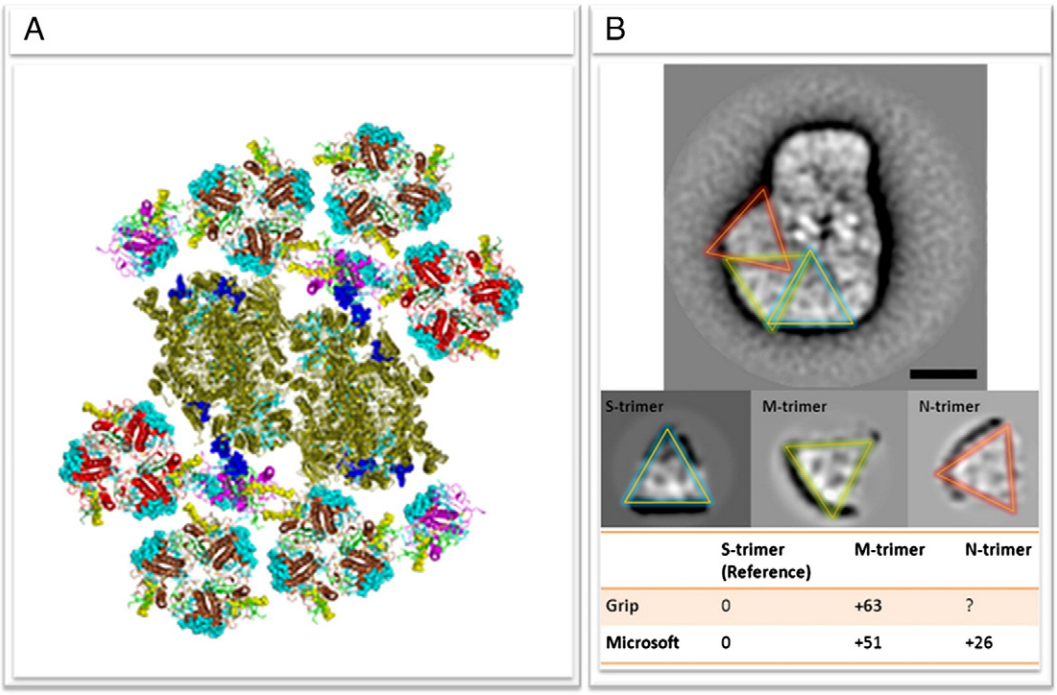

Fig. 4. Panel A: model of the structure of the *C.r.* PSII–LHCII supercomplex. The model has been assembled based on the projection map in Fig. 2 using the crystal structures of the cyanobacterial PSII core [6] (3ARC), LHCII trimer [13] (1RWT) and CP29 [16] (3PL9). For CP26, the structure of a monomeric LHCII has been used. Proteins of the PSII core (lime green), LHCII-S and -M (brown), novel LHCII-N (red), CP29 and CP26 (magenta), Chls a (cyan), Chls b (green), neoxanthin (yellow spheres), lutein L1 (orange), lutein L2 (dark-yellow sticks). Panel B: presentation of LHCII-S, LHCII-M and LHCII-N trimers selected from the *C.r.* C_2S_2MN PSII supercomplex to determine their rotated orientations. S-trimer orientation was used as a reference.

of C2S complexes in this fraction. Because of the high sequence identity between the *LhcbM* proteins, it was not possible to use spectral counts to determine their relative amount in the three samples. However, the number of unique spectra matched to the different *LhcbM* types is very different and implies that *LhcbM2*/*7*, *LhcbM1* and *LhcbM3* are the most abundant *LhcbM* proteins in this alga.

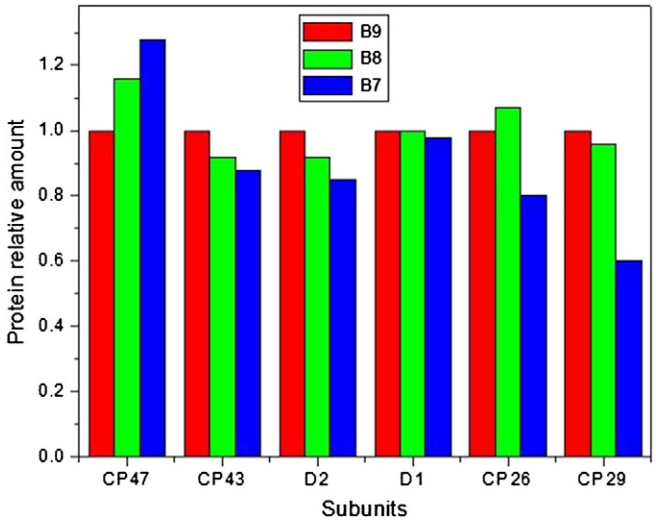

Fig. 5. Protein composition of PSII–LHCII supercomplexes. The number of spectra assigned to individual PSII core subunits and *Lhcb* monomers (CP26 and CP29) was normalized to the average number of spectra assigned to the core complex polypeptides (calculated as (D1 + D2) / 2) in the same fraction. The values are reported relatively to the values determined for each polypeptide in fraction B9.

3.4. Pigment composition

The pigment composition of fractions B2, B3 and B7–B9, was analyzed together with the composition of *C. reinhardtii* cells. The results are reported in Table 1.

A Chl a/b ratio of 1.29 and 1.28 was obtained for the fractions of monomeric (B2) and trimeric (B3) antenna complexes, similar to what was previously observed [51] slightly lower than the value of plant LHCII (1.33). The trimer coordinates four carotenoids per 14 Chls as it is the case in plants. The carotenoid composition of *C. reinhardtii* is considered to be similar to that of higher plants [52] with the addition of loroxanthin, which derives from lutein by hydroxylation of the methyl group at C9 of the polyene chain and is selectively bound to LHCII [53,54]. Indeed in the trimeric fraction we observed the presence of loroxanthin and a lower content of lutein as compared to higher plant LHCII [52]. Although it was not possible to fully separate neoxanthin from loroxanthin, the fact that all *LhcbMs* contain the tyrosine responsible for the selectivity of the N1 binding site for neoxanthin [55], suggests the binding of 1 neoxanthin per complex and thus of around 0.7 loroxanthin per monomer. Loroxanthin is probably substituting lutein in one of the two internal binding sites (L1 and L2).

3.5. Spectroscopic characterization

The absorption spectra of fractions B2–B9 were measured at room temperature and are presented in Fig. 6. The spectra of fractions B2 and B3 (Fig. 6A) show maxima at 672 nm and at 670 nm respectively. Interestingly the absorption maximum of the *C.r.* LHCII trimer is 4 nm blue shifted compared to that of the complex of higher plants (Fig. 6B) and it shows relatively more intense absorption around 650–653 nm, in agreement with the lower Chl a/b ratio.

The absorption spectra of fractions B7–B9 (Fig. 6C) showed maxima at 675 nm. A relative increase in intensity of the absorption in the Chl b

Table 1
Pigment composition of: LHCII monomers (B2), trimers (B3) and *C.r.* PSII supercomplexes (B7–B9). The values of individual carotenoids are normalized to 14 Chls (a + b) in fractions B3 and to 100 Chls (a + b) in fractions with PSII supercomplexes (B7–B9) and thylakoids. The data are the results of at least four different preparations in two replicas.

	Chl a/Chl b	Chls/Cars	Neoxanthin/loroxanthin	Violaxanthin	Lutein	β-Carotene
B2	1.29 ± 0.06	3.79 ± 0.54	2.41 ± 0.20	0.55 ± 0.07	0.91 ± 0.04	–
B3 (LHCII trimer)	1.28 ± 0.02	3.65 ± 0.11	1.67 ± 0.22	0.68 ± 0.05	1.44 ± 0.18	–
B7	2.94 ± 0.18	5.60 ± 0.39	5.75 ± 0.48	1.01 ± 0.09	5.42 ± 0.47	5.65 ± 0.50
B8	2.41 ± 0.17	4.80 ± 0.75	6.98 ± 0.93	1.03 ± 0.09	6.43 ± 0.91	6.40 ± 1.04
B9	2.22 ± 0.13	4.67 ± 0.38	7.09 ± 0.42	1.12 ± 0.11	8.57 ± 1.44	7.11 ± 1.92
C.r. cells	2.28 ± 0.061	4.51 ± 0.421	–	–	–	–

region (630–660 nm) was observed going from B7 to B9 (Fig. 6C), in agreement with the increased antenna size of the supercomplexes.

To check the integrity of PSII supercomplexes, fluorescence spectra from fractions B7–B9 were measured at 5 °C (Fig. 7A). The maximum emission for all fractions was at 678 nm. The perfect overlapping of the emission spectra after excitation at 440 nm, 475 nm and 500 nm, which excite preferentially Chl a, Chl b and carotenoids, indicates that there are no free pigments in these preparations. In Fig. 6A only the emission spectra of B9 are shown, but the results were very similar for all fractions.

Low temperature (77 K) fluorescence emission spectra showed a major peak at 676 nm in all three fractions and a shoulder at 690–700 nm which is likely due to the core complex (Fig. 7B). Moreover, the spectrum of the supercomplexes is clearly red-shifted as compared to that of LHCII trimer, confirming that there is energy transfer between LHCII and the core.

4. Discussion

4.1. In the C. reinhardtii PSII supercomplex LHCII-N trimer substitutes CP24 and stabilizes the binding of trimer M (and the other way around)

Early work comparing a PSII supercomplex isolated from *C. reinhardtii* with the C_2S_2 supercomplex of spinach showed high similarity in shape and size [7]. This, together with the fact that CP24, which is essential for the binding of trimer M in plants [3,35,36], is absent in *C. reinhardtii* led to the conclusion that the PSII supercomplex of this alga is organized as C_2S_2. Recently, larger complexes were observed containing a novel trimer (here called N) in addition to trimers S and M [33]. In our study, the EM analysis of isolated *C.r.* PSII supercomplexes (B7–B9) showed that they were present in $C_2S_2M_2N_2$, C_2S_2MN, C_2SMN and C_2S_2 configurations, while differently from higher plants, no C_2S_2M, C_2SM, $C_2S_2M_2$ or C_2M [3] could be found. Apparently, the lack of the neighboring N-trimer strongly influences the binding of LHCII-M, as does CP24 in plants. Indeed in higher plants a complex composed of CP24/CP29/LHCII could be isolated [56], indicating that the association between these proteins is stronger than between them and the core. The CP24/CP29/LHCII complex is obviously not present in *C. reinhardtii*, but the analysis of the sucrose gradient bands indicates the presence of a CP29/LHCII-M/LHCII-N complex. This suggests that the connection of trimers N and M is stronger than their association with the core and might also explain why, after detergent solubilization, only C_2S_2 could be detected in early works [7,34].

These results point out that the hypothesis that CP24 has evolved in land plants to increase the antenna size of PSII (or to avoid the formation of C2S2) should be reconsidered as clearly PSII–LHCII of *C. reinhardtii* is larger than the largest supercomplex of plants [35,36]. It has been shown that under high light stress CP24 and LHCII-M dissociate from the supercomplex [57]. It is thus likely that CP24 (and *Lhcb3*) has evolved not to make the antenna size of PSII larger, but more flexible, allowing for a fast regulation of the PSII antenna size.

4.2. LhcbM1, LhcbM2/7 and LhcbM3 are the main components of the PSII supercomplexes while LhcbM5 is enriched in the "extra" LHCII population

LHCII antenna in *C. reinhardtii* is codified by 9 different genes, *LhcbM1–M9*, but very little is known about their organization and occurrence. The possibility to compare the composition of supercomplexes containing different trimers (S for B7 and B8 and S, M and N for B9) with that of the LHCII trimers that were detached from the supercomplexes (B3) allows to analyze the protein composition of each trimer. Four main *LhcbM* bands could be resolved in SDS-PAGE, which were identified as the four types of *LhcbM* complexes. It is interesting to observe that, while the ratio *LhcbM*/core is increasing when

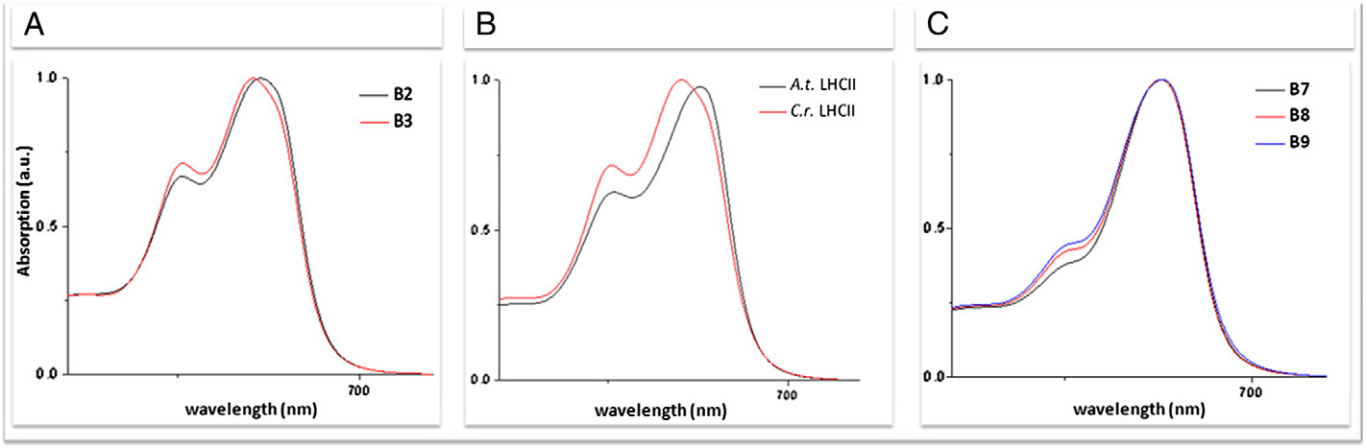

Fig. 6. Absorption spectra at room temperature of the fractions from sucrose gradient. The spectra were normalized to the maximum absorption of the Qy region. Panel A: absorption spectra of fractions B2 and B3. Panel B: comparison of the absorption spectra of *C.r.* LHCII and *A.t.* LHCII trimers. C: absorption spectra of fractions B7–B9.

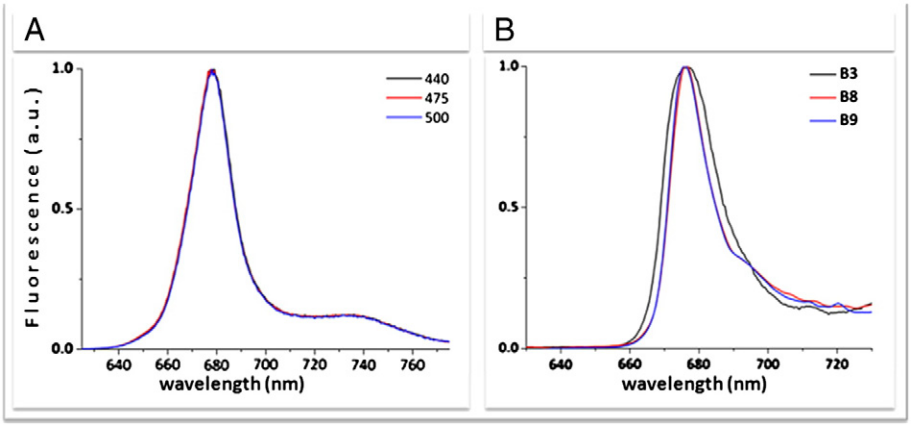

Fig. 7. Fluorescence emission spectra of the PSII–LHCII supercomplexes. Panel A: fluorescence emission spectra of PSII–LHCII supercomplex from B9 fraction recorded at 5 °C. Panel B: low temperature (77 K) fluorescence emission spectra of PSII–LHCII supercomplexes (B8–B9) and *C.r.* LHCII trimers (B3) excited at 440 nm.

going from B7 to B9, the relative abundance of the bands associated with Types I, IV and III polypeptides remains the same. This suggests that all trimers, have similar protein composition wherein *LhcbM1*, *LhcbM2/7* and *LhcbM3* are the dominant proteins, as confirmed by mass spectrometry identification. Interestingly the SDS-PAGE shows that *LhcbM5* is highly enriched in B3, while very little *LhcbM5* is present in the supercomplexes, suggesting that it is mainly present in the LHCII pool that is not directly associated with the core and that in plants we have defined as "extra" LHCII [58]. In addition, *LhcbM5*, together with *LhcbM1*, is the only protein that conserves the phosphorylation site which is important for state transitions [21] and it has indeed been proposed to participate in this process [27,59].

4.3. The properties of C.r. LHCII differ from those of plant LHCII

Sequence analysis has shown that the *LhcbM* proteins of *C. reinhardtii* do not exactly correlate with the *Lhcb1*–3 proteins of higher plants [21,24] although they show a high degree of identity. All amino acids which were shown to be responsible for the Chl binding in plants [13] are conserved in the nine *LhcbM* proteins suggesting that they bind the same number of Chls as the complexes from plants. The Chl a/b ratio of the trimer differs only very slightly from that of plants (1.28 in *C. reinhardtii* vs. 1.33 in plants) indicating at most the change of affinity of one binding site. However, the absorption spectrum of *C.r.* LHCII trimer is different from that of *A.t.* LHCII (Fig. 6B) showing a blue shifted maximum. This difference is not due to changes in the lowest energy pigments, but rather in the environment of Chls absorbing around 674 nm, which in plants are located in the 602 and 603 binding sites [60].

4.4. Energy transfer in PSII–LHCII of C. reinhardtii

The role of LHCII is to absorb light and to transfer excitation energy to the reaction center where charge separation occurs. The connection of LHCII trimers with the core is thus essential in assuring efficient energy transfer [2]. In plants it has been shown that the overall trapping time in the PSII supercomplex is 143 ps [61] and that this very fast transfer is probably due to the presence of preferential energy transfer pathways between complexes involving mainly Chls a. The reconstituted structure of the *C.r.* PSII supercomplex gives the possibility to point out preferential energy transfer pathways, based on the organization of the Chls. The model of the supercomplex shows that the relative orientation of the S trimer is identical to that in higher plants, which means that chlorophylls 610–611–612 (nomenclature from [13]) of one LHCII monomer, are close to Chl 633 of the core, (nomenclature from [6]), allowing for rapid energy transfer as in plants. The orientation of trimer M is different than in *A. thaliana*. In this configuration Chls a 610 and 604 of LHCII face directly CP29, while Chls 611 and 612 of a different monomer face trimer N. In the case of trimer N the shorter Chl (LHCII)–Chl (core) distance (around 20 Å) is between Chls 611 and 612 of one LHCII trimer and Chl 612 of the core. In conclusion, also in the case of *C. reinhardtii* Chls 610–612 seem to be involved in the transfer between complexes, although the connection between trimer M and CP29 involves Chl 610 instead of Chls 611 and 612 as in *A. thaliana*. These Chls represent the lowest energy sites in LHCII of plants [60,62] and they are likely to be conserved also in *C. reinhardtii*. The minimal distance between Chls in trimer N and in the core is rather large, suggesting a slower transfer, although at this stage we cannot exclude that an additional Chl could be located in between these two complexes in *C. reinhardtii*.

4.5. The thylakoid membrane of C. reinhardtii harbors at least 6 LHCII trimers per monomeric PSII core complex

The fraction containing the largest PSII supercomplex has a Chl a/b ratio of 2.22, in perfect agreement with the presence of 3.7 trimers on average per dimeric core complex in this fraction. This number is very close to the Chl a/b ratio of *C. reinhardtii* cells which is 2.28. However, the cells also contain PSI in a close to 1:1 stoichiometry with PSII, in agreement with previous studies [46,63–65]. Considering that PSI coordinates around 240 Chls, 196 Chl a and 44 Chl b [40], the low Chl a/b ratio of the cells can only be explained with the presence of extra LHCII trimers in the photosynthetic membrane of *C. reinhardtii.* The number can be roughly calculated on the basis of the pigment stoichiometry of core (35 Chls a) and PSII antennas [66]. We have used 14 Chls a value of 1.28 for the Chl a/b (than 7.85 Chl a and 6.15 Chl b) of all antenna complexes, although it is probably on the low side for CP29 and CP26, which means that we underestimate the number of LHCII trimers. The number X of antenna (monomers) is thus calculated as $2.28 = (196 + 35 + 7.85X) / (44 + 6.15X)$. The result suggests the presence of 3–4 additional LHCII trimers per monomeric core (meaning 6/7 in total), making the light harvesting capacity of *C. reinhardtii* far larger than that of plants, in which a maximum of 4.5 LHCII trimers was observed [67,68]. Where are the additional trimers located? Looking at the structure of the PSII supercomplex it is clear that there is space at most for one extra trimer associated with the core. The tighter possible organization of the PSII supercomplexes of *C. reinhardtii* is shown in Fig. 8 and indicates that differently from the case of plants the dimeric cores cannot be directly connected but are separated by a minimum of one row of LHCII. In this case we can speculate that trimer N should be able to transfer energy to two different core complexes.

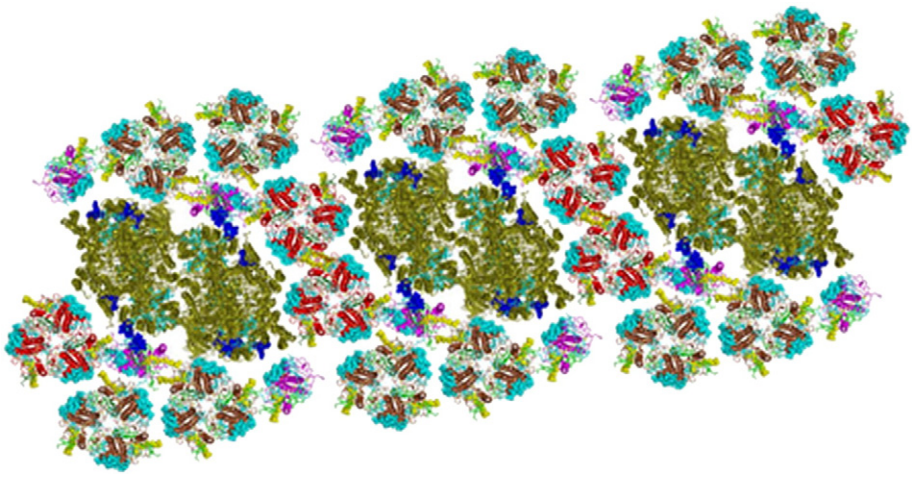

Fig. 8. Model of the tighter possible organization of the $C_2S_2M_2N_2$ supercomplexes of *Chlamydomonas*.

It remains to be elucidated if the "extra" trimers are located in between the PSII supercomplexes and if a subpopulation of them is associated with PSI in all conditions, as it is the case in plants [58] or if they form LHCII-only domains.

Supplementary data to this article can be found online at http://dx.doi.org/10.1016/j.bbabio.2013.07.012.

Acknowledgements

We thank Kevin Redding (Arizona State University, Tempe, USA) for kindly providing the *C. reinhardtii* strain (JVD-1B [pGG1]) used in this work and Pierre Cardol (Université de Liège) for his help with the ECS measurements. This work was supported by the ERC Starting Grant 281341 (ASAP) to RC and FOM Grant 10TBSC12-2 to EJB.

References

[1] C. Goussias, A. Boussac, A.W. Rutherford, Photosystem II and photosynthetic oxidation of water: an overview, Philos. Trans. R. Soc. B 357 (2002) 1369–1381.
[2] R. Croce, H. van Amerongen, Light-harvesting and structural organization of Photosystem II: from individual complexes to thylakoid membrane, J. Photochem. Photobiol. B 104 (2011) 142–153.
[3] S. Caffarri, R. Kouril, S. Kereiche, E.J. Boekema, R. Croce, Functional architecture of higher plant Photosystem II supercomplexes, EMBO J. 28 (2009) 3052–3063.
[4] L.X. Shi, M. Hall, C. Funk, W.P. Schroder, Photosystem II, a growing complex: updates on newly discovered components and low molecular mass proteins, BBA-Bioenergetics 1817 (2012) 13–25.
[5] J.P. Dekker, E.J. Boekema, Supramolecular organization of thylakoid membrane proteins in green plants, BBA-Bioenergetics 1706 (2005) 12–39.
[6] Y. Umena, K. Kawakami, J.R. Shen, N. Kamiya, Crystal structure of oxygen-evolving Photosystem II at a resolution of 1.9 angstrom, Nature 473 (2011) 55–U65.
[7] J. Nield, O. Kruse, J. Ruprecht, P. da Fonseca, C. Buchel, J. Barber, Three-dimensional structure of *Chlamydomonas reinhardtii* and *Synechococcus elongatus* Photosystem II complexes allows for comparison of their oxygen-evolving complex organization, J. Biol. Chem. 275 (2000) 27940–27946.
[8] C. Buchel, W. Kuhlbrandt, Structural differences in the inner part of Photosystem II between higher plants and cyanobacteria, Photosynth. Res. 85 (2005) 3–13.
[9] H. Dau, I. Zaharieva, M. Haumann, Recent developments in research on water oxidation by Photosystem II, Curr. Opin. Chem. Biol. 16 (2012) 3–10.
[10] N.C. Dang, V. Zazubovich, M. Reppert, B. Neupane, R. Picorel, M. Seibert, R. Jankowiak, The CP43 proximal antenna complex of higher plant Photosystem II revisited: modeling and hole burning study I, J. Phys. Chem. B 112 (2008) 9921–9933.
[11] K. Ifuku, S. Ishihara, F. Sato, Molecular functions of oxygen-evolving complex family proteins in photosynthetic electron flow, J. Integr. Plant Biol. 52 (2010) 723–734.
[12] S. Jansson, A guide to the Lhc genes and their relatives in *Arabidopsis*, Trends Plant Sci. 4 (1999) 236–240.
[13] Z.F. Liu, H.C. Yan, K.B. Wang, T.Y. Kuang, J.P. Zhang, L.L. Gui, X.M. An, W.R. Chang, Crystal structure of spinach major light-harvesting complex at 2.72 angstrom resolution, Nature 428 (2004) 287–292.
[14] A. Ben-Shem, F. Frolow, N. Nelson, Crystal structure of plant Photosystem I, Nature 426 (2003) 630–635.
[15] R. Standfuss, A.C.T. van Scheltinga, M. Lamborghini, W. Kuhlbrandt, Mechanisms of photoprotection and nonphotochemical quenching in pea light-harvesting complex at 2.5 Å resolution, EMBO J. 24 (2005) 919–928.
[16] X.W. Pan, M. Li, T. Wan, L.F. Wang, C.J. Jia, Z.Q. Hou, X.L. Zhao, J.P. Zhang, W.R. Chang, Structural insights into energy regulation of light-harvesting complex CP29 from spinach, Nat. Struct. Mol. Biol. 18 (2011) 309–U394.
[17] R. Croce, G. Canino, F. Ros, R. Bassi, Chromophore organization in the higher-plant Photosystem II antenna protein CP26, Biochemistry-US 41 (2002) 7334–7343.
[18] F. Passarini, E. Wientjes, R. Hienerwadel, R. Croce, Molecular basis of light harvesting and photoprotection in CP24: unique features of the most recent antenna complex, J. Biol. Chem. 284 (2009) 29536–29546.
[19] S. de Bianchi, M. Ballottari, L. Dall'osto, R. Bassi, Regulation of plant light harvesting by thermal dissipation of excess energy, Biochem. Soc. Trans. 38 (2010) 651–660.
[20] P. Muller, X.P. Li, K.K. Niyogi, Non-photochemical quenching. A response to excess light energy, Plant Physiol. 125 (2001) 1558–1566.
[21] D. Elrad, A.R. Grossman, A genome's-eye view of the light-harvesting polypeptides of *Chlamydomonas reinhardtii*, Curr. Genet. 45 (2004) 61–75.
[22] J. Minagawa, Y. Takahashi, Structure, function and assembly of Photosystem II and its light-harvesting proteins, Photosynth. Res. 82 (2004) 241–263.
[23] S.S. Merchant, S.E. Prochnik, O. Vallon, E.H. Harris, S.J. Karpowicz, G.B. Witman, A. Terry, A. Salamov, L.K. Fritz-Laylin, L. Marechal-Drouard, W.F. Marshall, L.H. Qu, D.R. Nelson, A.A. Sanderfoot, M.H. Spalding, V.V. Kapitonov, Q.H. Ren, P. Ferris, E. Lindquist, H. Shapiro, S.M. Lucas, J. Grimwood, J. Schmutz, P. Cardol, H. Cerutti, G. Chanfreau, C.L. Chen, V. Cognat, M.T. Croft, R. Dent, S. Dutcher, E. Fernandez, H. Fukuzawa, D. Gonzalez-Ballester, D. Gonzalez-Halphen, A. Hallmann, M. Hanikenne, M. Hippler, W. Inwood, K. Jabbari, M. Kalanon, R. Kuras, P.A. Lefebvre, S.D. Lemaire, A.V. Lobanov, M. Lohr, A. Manuell, I. Meir, L. Mets, M. Mittag, T. Mittelmeier, J.V. Moroney, J. Moseley, C. Napoli, A.M. Nedelcu, K. Niyogi, S.V. Novoselov, I.T. Paulsen, G. Pazour, S. Purton, J.P. Ral, D.M. Riano-Pachon, W. Riekhof, L. Rymarquis, M. Schroda, D. Stern, J. Umen, R. Willows, N. Wilson, S.L. Zimmer, J. Allmer, J. Balk, K. Bisova, C.J. Chen, M. Elias, K. Gendler, C. Hauser, M.R. Lamb, H. Ledford, J.C. Long, J. Minagawa, M.D. Page, J.M. Pan, W. Pootakham, S. Roje, A. Rose, E. Stahlberg, A.M. Terauchi, P.F. Yang, S. Ball, C. Bowler, C.L. Dieckmann, V.N. Gladyshev, P. Green, R. Jorgensen, S. Mayfield, B. Mueller-Roeber, S. Rajamani, R.T. Sayre, P. Brokstein, I. Dubchak, D. Goodstein, L. Hornick, Y.W. Huang, J. Jhaveri, Y.G. Luo, D. Martinez, W.C.A. Ngau, B. Otillar, A. Poliakov, A. Porter, L. Szajkowski, G. Werner, K.M. Zhou, I.V. Grigoriev, D.S. Rokhsar, A.R. Grossman, C. Annotation, J.A. Team, The *Chlamydomonas* genome reveals the evolution of key animal and plant functions, Science 318 (2007) 245–251.
[24] H. Teramoto, T. Ono, J. Minagawa, Identification of *Lhcb* gene family encoding the light-harvesting Chlorophyll-a/b proteins of Photosystem II in *Chlamydomonas reinhardtii*, Plant Cell Physiol. 42 (2001) 849–856.
[25] D. Elrad, K.K. Niyogi, A.R. Grossman, A major light-harvesting polypeptide of Photosystem II functions in thermal dissipation, Plant Cell 14 (2002) 1801–1816.
[26] P. Ferrante, M. Ballottari, G. Bonente, G. Giuliano, R. Bassi, *LHCBM1* and *LHCBM2/7* polypeptides, components of major LHCII complex, have distinct functional roles in photosynthetic antenna system of *Chlamydomonas reinhardtii*, J. Biol. Chem. 287 (2012) 16276–16288.
[27] H. Takahashi, M. Iwai, Y. Takahashi, J. Minagawa, Identification of the mobile light-harvesting complex II polypeptides for state transitions in *Chlamydomonas reinhardtii*, Proc. Natl. Acad. Sci. U. S. A. 103 (2) (2006) 477–482.
[28] A. Guskov, J. Kern, A. Gabdulkhakov, M. Broser, A. Zouni, W. Saenger, Cyanobacterial Photosystem II at 2.9-angstrom resolution and the role of quinones, lipids, channels and chloride, Nat. Struct. Mol. Biol. 16 (2009) 334–342.
[29] E.J. Boekema, H. van Roon, J.F.L. van Breemen, J.P. Dekker, Supramolecular organization of Photosystem II and its light-harvesting antenna in partially solubilized Photosystem II membranes, Eur. J. Biochem. 266 (1999) 444–452.
[30] J. Nield, E.V. Orlova, E.P. Morris, B. Gowen, M. van Heel, J. Barber, 3D map of the plant Photosystem II supercomplex obtained by cryoelectron microscopy and single particle analysis, Nat. Struct. Biol. 7 (2000) 44–47.
[31] A.E. Yakushevska, P.E. Jensen, W. Keegstra, H. van Roon, H.V. Scheller, E.J. Boekema, J.P. Dekker, Supermolecular organization of Photosystem II and its associated

light-harvesting antenna in *Arabidopsis thaliana*, Eur. J. Biochem. 268 (2001) 6020–6028.
[32] A.E. Yakushevska, W. Keegstra, E.J. Boekema, J.P. Dekker, J. Andersson, S. Jansson, A.V. Ruban, P. Horton, The structure of Photosystem II in *Arabidopsis*: localization of the CP26 and CP29 antenna complexes, Biochemistry-US 42 (2003) 608–613.
[33] R. Tokutsu, N. Kato, K.H. Bui, T. Ishikawa, J. Minagawa, Revisiting the supramolecular organization of Photosystem II in *Chlamydomonas reinhardtii*, J. Biol. Chem. 287 (2012) 31574–31581.
[34] M. Iwai, Y. Takahashi, J. Minagawa, Molecular remodeling of Photosystem II during state transitions in *Chlamydomonas reinhardtii*, Plant Cell 20 (2008) 2177–2189.
[35] L. Kovacs, J. Damkjaer, S. Kereiche, C. Ilioaia, A.V. Ruban, E.J. Boekema, S. Jansson, P. Horton, Lack of the light-harvesting complex CP24 affects the structure and function of the grana membranes of higher plant chloroplasts, Plant Cell 18 (2006) 3106–3120.
[36] S. de Bianchi, L. Dall'Osto, G. Tognon, T. Morosinotto, R. Bassi, Minor antenna proteins CP24 and CP26 affect the interactions between Photosystem II subunits and the electron transport rate in grana membranes of *Arabidopsis*, Plant Cell 20 (2008) 1012–1028.
[37] G. Gulis, K.V. Narasimhulu, L.N. Fox, K.E. Redding, Purification of His(6)-tagged Photosystem I from *Chlamydomonas reinhardtii*, Photosynth. Res. 96 (2008) 51–60.
[38] D.S. Gorman, R.P. Levine, Cytochrome f and plastocyanin: their sequence in the photosynthetic electron transport chain of *Chlamydomonas reinhardi*, Proc. Natl. Acad. Sci. U. S. A. 54 (1965) 1665–1669.
[39] N. Fischer, P. Setif, J.D. Rochaix, Targeted mutations in the psaC gene of *Chlamydomonas reinhardtii*: preferential reduction of F-B at low temperature is not accompanied by altered electron flow from Photosystem I ferredoxin, Biochemistry-US 36 (1997) 93–102.
[40] B. Drop, M. Webber-Birungi, F. Fusetti, R. Kouril, K.E. Redding, E.J. Boekema, R. Croce, Photosystem I of *Chlamydomonas reinhardtii* contains nine light-harvesting complexes (Lhca) located on one side of the core, J. Biol. Chem. 286 (2011) 44878–44887.
[41] D.A. Berthold, G.T. Babcock, C.F. Yocum, A highly resolved, oxygen-evolving Photosystem-II preparation from spinach thylakoid membranes — electron-paramagnetic-resonance and electron-transport properties, FEBS Lett. 134 (1981) 231–234.
[42] R. Bassi, Spectral properties and polypeptide composition of the chlorophyll–proteins from thylakoids of granal and agranal chloroplasts of maize (*Zea-mays*-L), Carlsberg Res. Commun. 50 (1985) 127–143.
[43] R.J. Porra, W.A. Thompson, P.E. Kriedemann, Determination of accurate extinction coefficients and simultaneous-equations for assaying Chlorophyll-a and Chlorophyll-b extracted with 4 different solvents — verification of the concentration of chlorophyll standards by atomic-absorption spectroscopy, Biochim. Biophys. Acta 975 (1989) 384–394.
[44] D.G. Angeler, M. Schagerl, Distribution of the xanthophyll loroxanthin in selected members of the Chlamydomonadales and Volvocales (Chlorophyta), Phyton-Ann. Rei Bot. A 37 (1997) 119–132.
[45] P. Joliot, R. Delosme, Flash-induced 519 nm absorption change in green-algae, Biochim. Biophys. Acta 357 (1974) 267–284.
[46] D. Petroutsos, A.M. Terauchi, A. Busch, I. Hirschmann, S.S. Merchant, G. Finazzi, M. Hippler, PGRL1 participates in iron-induced remodeling of the photosynthetic apparatus and in energy metabolism in *Chlamydomonas reinhardtii*, J. Biol. Chem. 284 (2009) 32770–32781.
[47] B. Bailleul, P. Cardol, C. Breyton, G. Finazzi, Electrochromism: a useful probe to study algal photosynthesis, Photosynth. Res. 106 (2010) 179–189.
[48] G.T. Oostergetel, W. Keegstra, A. Brisson, Automation of specimen selection and data acquisition for protein electron crystallography, Ultramicroscopy 74 (1998) 47–59.
[49] R. Bassi, F.A. Wollman, The Chlorophyll-a/b proteins of Photosystem-II in *Chlamydomonas reinhardtii* — isolation, characterization and immunological cross-reactivity to higher-plant polypeptides, Planta 183 (1991) 423–433.
[50] H.B. Liu, R.G. Sadygov, J.R. Yates, A model for random sampling and estimation of relative protein abundance in shotgun proteomics, Anal. Chem. 76 (2004) 4193–4201.
[51] B. Pineau, C. Gerard-Hirne, C. Selve, Carotenoid binding to Photosystems I and II of *Chlamydomonas reinhardtii* cells grown under weak light or exposed to intense light, Plant Physiol. Biochem. 39 (2001) 73–85.
[52] R. Bassi, B. Pineau, P. Dainese, J. Marquardt, Carotenoid-binding proteins of Photosystem II, Eur. J. Biochem. 212 (1993) 297–303.
[53] A.R. Grossman, M. Lohr, C.S. Im, *Chlamydomonas reinhardtii* in the landscape of pigments, Annu. Rev. Genet. 38 (2004) 119–173.
[54] J. Knoetzel, T. Braumann, L.H. Grimme, Pigment–protein complexes of green-algae — improved methodological steps for the quantification of pigments in pigment–protein complexes derived from the green-algae *Chlorella* and *Chlamydomonas*, J. Photochem. Photobiol. B 1 (1988) 475–491.
[55] S. Caffarri, F. Passarini, R. Bassi, R. Croce, A specific binding site for neoxanthin in the monomeric antenna proteins CP26 and CP29 of Photosystem II, FEBS Lett. 581 (2007) 4704–4710.
[56] P. Dainese, R. Bassi, Subunit stoichiometry of the chloroplast Photosystem-II antenna system and aggregation state of the component Chlorophyll-a/b binding-proteins, J. Biol. Chem. 266 (1991) 8136–8142.
[57] N. Betterle, M. Ballottari, S. Zorzan, S. de Bianchi, S. Cazzaniga, L. Dall'Osto, T. Morosinotto, R. Bassi, Light-induced dissociation of an antenna hetero-oligomer is needed for non-photochemical quenching induction, J. Biol. Chem. 284 (2009) 15255–15266.
[58] E. Wientjes, H. van Amerongen, R. Croce, LHCII is an antenna of both photosystems after long-term acclimation, Biochim. Biophys. Acta 1827 (2013) 420–426.
[59] E.J. Stauber, A. Fink, C. Markert, O. Kruse, U. Johanningmeier, M. Hippler, Proteomics of *Chlamydomonas reinhardtii* light-harvesting proteins, Eukaryot Cell 2 (2003) 978–994.
[60] R. Remelli, C. Varotto, D. Sandona, R. Croce, R. Bassi, Chlorophyll binding to monomeric light-harvesting complex — a mutation analysis of chromophore-binding residues, J. Biol. Chem. 274 (1999) 33510–33521.
[61] S. Caffarri, K. Broess, R. Croce, H. van Amerongen, Excitation energy transfer and trapping in higher plant Photosystem II complexes with different antenna sizes, Biophys. J. 100 (2011) 2094–2103.
[62] V.I. Novoderezhkin, M.A. Palacios, H. Van Amerongen, R. van Grondelle, Excitation dynamics in the LHCII complex of higher plants: modeling based on the 2.72 angstrom crystal structure, J. Phys. Chem. B 109 (2005) 10493–10504.
[63] A. Melis, A. Murakami, J.A. Nemson, K. Aizawa, K. Ohki, Y. Fujita, Chromatic regulation in *Chlamydomonas reinhardtii* alters photosystem stoichiometry and improves the quantum efficiency of photosynthesis, Photosynth. Res. 47 (1996) 253–265.
[64] J.E.W. Polle, J.R. Benemann, A. Tanaka, A. Melis, Photosynthetic apparatus organization and function in the wild type and a Chlorophyll b-less mutant of *Chlamydomonas reinhardtii*. Dependence on carbon source, Planta 211 (2000) 335–344.
[65] C.Y. Yan, O. Schofield, Z. Dubinsky, D. Mauzerall, P.G. Falkowski, M.Y. Gorbunov, Photosynthetic energy storage efficiency in *Chlamydomonas reinhardtii*, based on microsecond photoacoustics, Photosynth. Res. 108 (2011) 215–224.
[66] S.W. Hogewoning, E. Wientjes, P. Douwstra, G. Trouwborst, W. van Ieperen, R. Croce, J. Harbinson, Photosynthetic quantum yield dynamics: from photosystems to leaves, Plant Cell 24 (2012) 1921–1935.
[67] B. van Oort, M. Alberts, S. de Bianchi, L. Dall'Osto, R. Bassi, G. Trinkunas, R. Croce, H. van Amerongen, Effect of antenna-depletion in Photosystem II on excitation energy transfer in *Arabidopsis thaliana*, Biophys. J. 98 (2010) 922–931.
[68] G.F. Peter, J.P. Thornber, Biochemical-composition and organization of higher-plant Photosystem-II light-harvesting pigment–proteins, J. Biol. Chem. 266 (1991) 16745–16754.